Volume 4, Issue 5, 2026

Frontier in Medical & Health Research

ISSN: (e) 3007-1607 (p) 3007-1593

INDIGENOUS FUNGAL CONSORTIA FROM PLASTIC-CONTAMINATED LANDFILLS OF FAISALABAD DEMONSTRATE POTENT POLYURETHANE-DEGRADING CAPABILITIES: ENZYMATIC MECHANISMS AND MYCOREMEDIATION POTENTIAL

Sumaira Fardous[1], Farina Jamil[*2], Hamza Rafeeq[3]

[1, *2,3] *Department of Biochemistry, Riphah International University, Faisalabad Campus, Pakistan*

[*2]farina.jamil@riphahfsd.edu.pk

DOI: https://doi.org/10.5281/zenodo.20622927

Keywords
Aspergillus fumigatus; Biodegradation; Esterase; Indigenous fungi; Mycoremediation; Polyurethane; Urethanase; Waste management

Article History
Received: 03 April 2026
Accepted: 15 May 2026
Published: 30 May 2026

Corresponding Author: *
Farina Jamil

Abstract

The persistent accumulation of polyurethane (PU) waste in landfills and natural ecosystems poses a severe environmental challenge, demanding sustainable bioremediation solutions. This study isolated, characterized, and evaluated indigenous fungi from five plastic-contaminated landfill sites in Faisalabad, Pakistan, for their polyurethane-degrading capabilities. A total of 87 morphologically distinct fungal isolates were obtained from 43 composite samples via enrichment culture on mineral salt medium with PU as the sole carbon source. Multi-stage screening primary (clear zone formation, degradation index ≥ 1.2) and secondary (weight loss ≥ 10% in liquid culture over 60 days) identified 12 potent degraders meeting stringent tertiary criteria (DI ≥ 1.5; weight loss ≥ 15%). Molecular identification via ITS region sequencing revealed diverse genera: Aspergillus (six species), Fusarium oxysporum, Penicillium chrysogenum, Alternaria alternata, A. tenuissima, Mucor circinelloides, and M. racemosus. A 120-day time-course study showed Aspergillus fumigatus KHF-05 achieved the highest weight loss (39.8%), followed by A. terreus KHF-12 (38.2%) and Fusarium oxysporum JRF-08 (34.5%). FTIR spectroscopy confirmed cleavage of ester carbonyl and urethane linkages; SEM documented extensive surface erosion, hyphal penetration, and biofilm formation. Peak extracellular enzyme activities were: esterase 1.42 U/mg, protease 0.82 U/mg, and urethanase 7.8 × 10^{-3} U/mg, with Pearson correlations to weight loss of r = 0.91, 0.67, and 0.88, respectively, confirming ester-bond hydrolysis as the primary mechanism.

1. INTRODUCTION

The exponential growth of global plastic production now exceeding 400 million metric tons annually has created one of the most pressing environmental crises of the contemporary era. Among synthetic polymers, polyurethane (PU) holds a singular industrial position due to its extraordinary versatility: flexible foams in furniture and bedding, rigid insulation panels, elastomers in automotive components, coatings, and adhesives. The global PU market, valued at USD 86.28 billion in 2024, is projected to reach USD 128.95 billion by 2034 (CAGR 4.10%), reflecting its irreplaceable industrial role.

Despite its utility, PU's chemical stability renders it highly resistant to natural degradation, contributing to long-term soil and aquatic pollution, microplastic contamination, and landfill overflow. Approximately 30% of recovered PU foam is consigned to landfills, and only one-

Frontier in Medical & Health Research

ISSN: (e) 3007-1607 (p) 3007-1593

third is effectively recycled. Conventional disposal methods mechanical recycling, hydrolysis, glycolysis, pyrolysis require harsh operating conditions, specialized infrastructure, and generate hazardous by-products, underscoring the urgent need for eco-friendly alternatives.

Mycoremediation the strategic deployment of fungi to remediate environmental contaminants offers compelling advantages: ambient-condition operation, minimal hazardous by-products, potential for complete polymer mineralization, and the capacity of fungal mycelial networks to physically colonize solid polymer matrices. Diverse fungal species including Aspergillus fumigatus, A. tubingensis, Penicillium chrysogenum, Fusarium solani, and the anaerobe-capable endophyte Pestalotiopsis microspora have demonstrated significant PU-degrading activity. However, most published studies have employed laboratory strains rather than indigenous isolates pre-adapted to local conditions a critical gap limiting both ecological relevance and practical applicability.

Pakistan, with rapidly urbanizing industrial cities facing acute plastic waste management challenges, represents an understudied geographic context for mycoremediation research. This study therefore aimed to: (i) isolate indigenous PU-degrading fungi from plastic-contaminated landfills in Faisalabad; (ii) quantitatively assess their degradation efficiency via weight loss analysis, FTIR spectroscopy, and SEM examination; and (iii) elucidate the enzymatic mechanisms esterase, protease, and urethanase underpinning PU biodegradation, providing a foundation for scalable mycoremediation strategies.

2. MATERIALS AND METHODS

2.1 Study Area and Sample Collection

Sampling was conducted post-monsoon at five landfill sites in Faisalabad, Punjab, Pakistan (Table 1), selected based on their documented history of plastic waste accumulation. At each site, composite soil samples (5–15 cm depth) and visibly colonized PU foam fragments were collected with sterilized tools, transported at ~4°C, and processed immediately upon arrival at the laboratory. Fifteen sampling points across five sites yielded 43 total samples.

Table 1. Description of sampling sites in Faisalabad for collection of plastic-contaminated soil and polyurethane waste.

Site	Location	Coordinates	Characteristics	Waste Type	Points
1	Jhumra Road	31.53°N 73.20°E	Active municipal landfill (15+ yrs)	Household plastics, PU foam	4
2	Khurrianwala	31.51°N 73.19°E	Industrial disposal, textile zone (12 yrs)	PU foam offcuts, coated fabrics	4
3	Satiana Road	31.39°N 73.11°E	Recently established landfill (6 yrs)	Household plastics, PU products	3
4	Chak Jhumra	31.57°N 73.18°E	Semi-controlled, mixed rural (10 yrs)	Agricultural plastic, PU foam	2
5	Sammundri Road	31.43°N 73.09°E	Uncontrolled open dump (8 yrs)	Mixed plastics, PU materials	2

2.2 Fungal Isolation and Screening

Enrichment culture: 10 g of each soil sample was incubated in mineral salt medium (MSM; pH 5.5) with 0.5% w/v powdered PU foam as the sole carbon source (28°C, 150 rpm, 21 days; one transfer). Serial dilutions were plated on PU-emulsified MSM agar. Direct plating: air-dried soil and foam fragments were placed onto selective MSM agar containing 50 µg/mL

Frontier in Medical & Health Research

ISSN: (e) 3007-1607 (p) 3007-1593

chloramphenicol. Colonies were subcultured ≥ 3 times on PDA for purification.

Primary screening: all 87 isolates were inoculated onto PU-emulsified MSM agar plates. A Degradation Index (DI = clear zone diameter / colony diameter) ≥ 1.2 after 21 days was the selection threshold. Secondary screening: 42 selected isolates were incubated with pre-weighed sterile PU films (Estane 5703; 2 × 2 cm; ~100 µm thick) in MSM (28°C, 120 rpm, 60 days). Percent weight loss = [(initial − final weight) / initial weight] × 100. Tertiary selection criteria: DI ≥ 1.5, weight loss ≥ 15%, robust PU-supported growth

2.3 Identification and Phylogenetics

Macroscopic and microscopic features were documented on PDA (7–14 days, 28°C). The ITS1–5.8S–ITS2 region was amplified from extracted genomic DNA using universal primers ITS1 and ITS4 (55°C annealing; 550–650 bp product), sequenced bidirectionally, and BLAST-searched against NCBI GenBank. Phylogenetic trees were constructed by neighbor-joining with Kimura 2-parameter model (1000 bootstrap replicates; ClustalW alignment).

2.4 Degradation Assessment and Enzyme Assays

The 12 selected isolates were incubated with sterile PU films in MSM for 120 days at 28°C with 120 rpm shaking. Weight loss was measured at 15-day intervals (triplicate flasks). FTIR spectra (ATR; 4000–400 cm^{-1}; 4 cm^{-1} resolution) and SEM (5–10 kV; gold-palladium coated; 500–5000×) assessed structural changes. Extracellular esterase was assayed with p-nitrophenyl acetate (405 nm; 1 unit = 1 µmol p-NP/min); protease with azocasein (440 nm); urethanase with ethyl carbamate via ammonia release (625 nm). Pearson correlations were calculated between peak enzyme activities and 120-day weight loss. ANOVA with Tukey's HSD ($p < 0.05$) was used throughout.

3. RESULTS

3.1 Isolation and Distribution of Fungal Isolates

A total of 87 fungal isolates were obtained from 43 samples across five landfill sites (Table 2). The Khurrianwala Industrial Waste Site yielded the highest number (n = 33), consistent with its prolonged exposure to PU waste from adjacent furniture manufacturing. Jhumra Road contributed 26 isolates; Satiana Road (16), Chak Jhumra (8), and Sammundri Road (4) yielded progressively fewer. Direct plating (n = 45) marginally outperformed enrichment culture (n = 42), confirming the complementarity of both approaches.

Table 2. Distribution of 87 fungal isolates across five sampling sites and two isolation methods.

Sampling Site	Samples	Enrichment	Direct Plating	Total
Jhumra Road Dumping Ground	12	12	14	26
Khurrianwala Industrial Waste	14	15	18	33
Satiana Road Municipal Landfill	8	8	8	16
Chak Jhumra Waste Area	5	4	4	8
Sammundri Road Open Dump	4	3	1	4
Total	**43**	**42**	**45**	**87**

Volume 4, Issue 5, 2026

Frontier in Medical & Health Research

ISSN: (e) 3007-1607 (p) 3007-1593

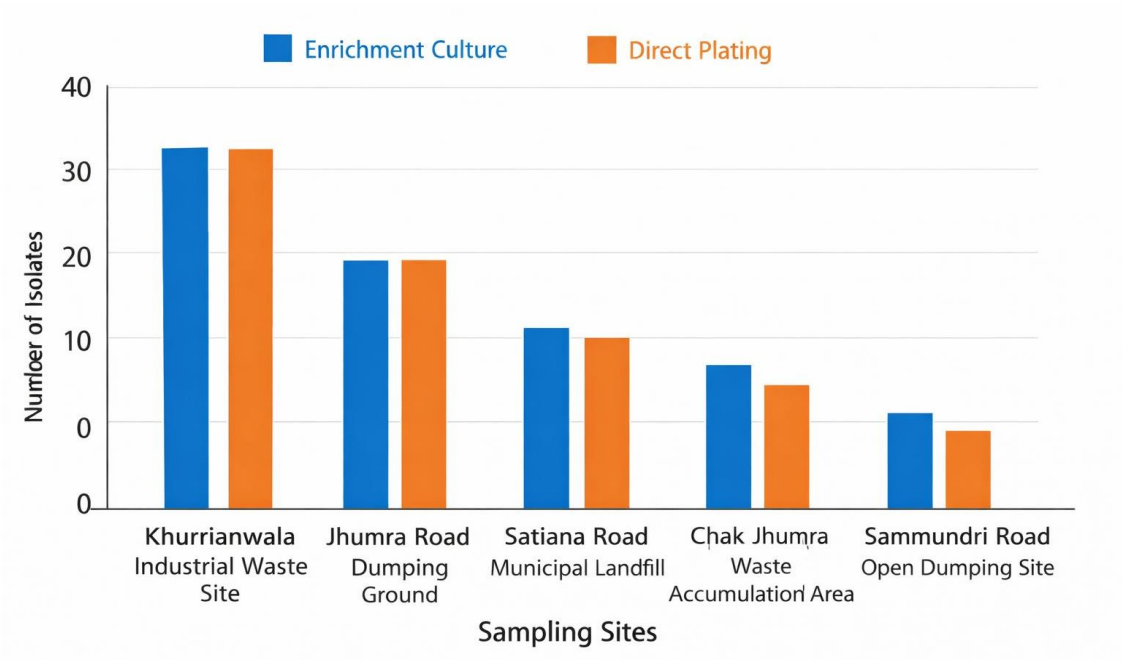

Figure 1. Distribution of 87 fungal isolates obtained from five different landfill sites in Faisalabad, showing the contribution of enrichment culture and direct plating methods to the total isolates per site.

3.2 Primary and Secondary Screening

Primary screening on PU-emulsified agar identified 42 of 87 isolates (48.3%) with DI ≥ 1.2, including 18 excellent degraders (DI 1.5–2.0) and 24 good degraders (DI 1.2–1.4) (Table 3). Secondary liquid-culture screening over 60 days narrowed the pool to 24 isolates (≥ 10% weight loss), of which 8 showed ≥ 15% weight loss. Tertiary selection yielded 12 isolates for detailed characterization.

Table 3. Primary screening results: distribution of 87 isolates by degradation index (DI) category.

DI Range	No. Isolates	% Total	Category
0.0 – 0.5	28	32.2%	Non-degraders / Weak
0.6 – 1.1	17	19.5%	Moderate degraders
1.2 – 1.4	24	27.6%	Good degraders (selected)
1.5 – 2.0	18	20.7%	Excellent degraders (selected)
Total	**87**	**100%**	**—**

Frontier in Medical & Health Research

ISSN: (e) 3007-1607 (p) 3007-1593

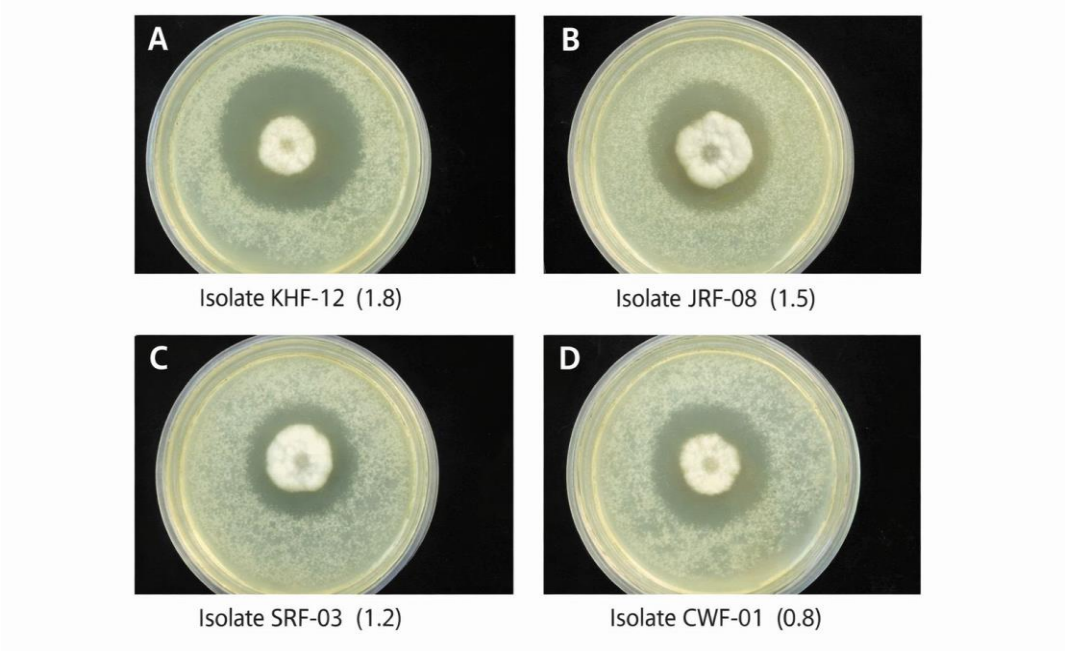

Figure 2. Primary screening of fungal isolates showing clear zone formation on polyurethane-emulsified agar plates after 14 days of incubation at 28°C. (A) KHF-12 with DI 1.8, (B) JRF-08 with DI 1.5, (C) SRF-03 with DI 1.2, (D) CWF-01 with DI 0.8.

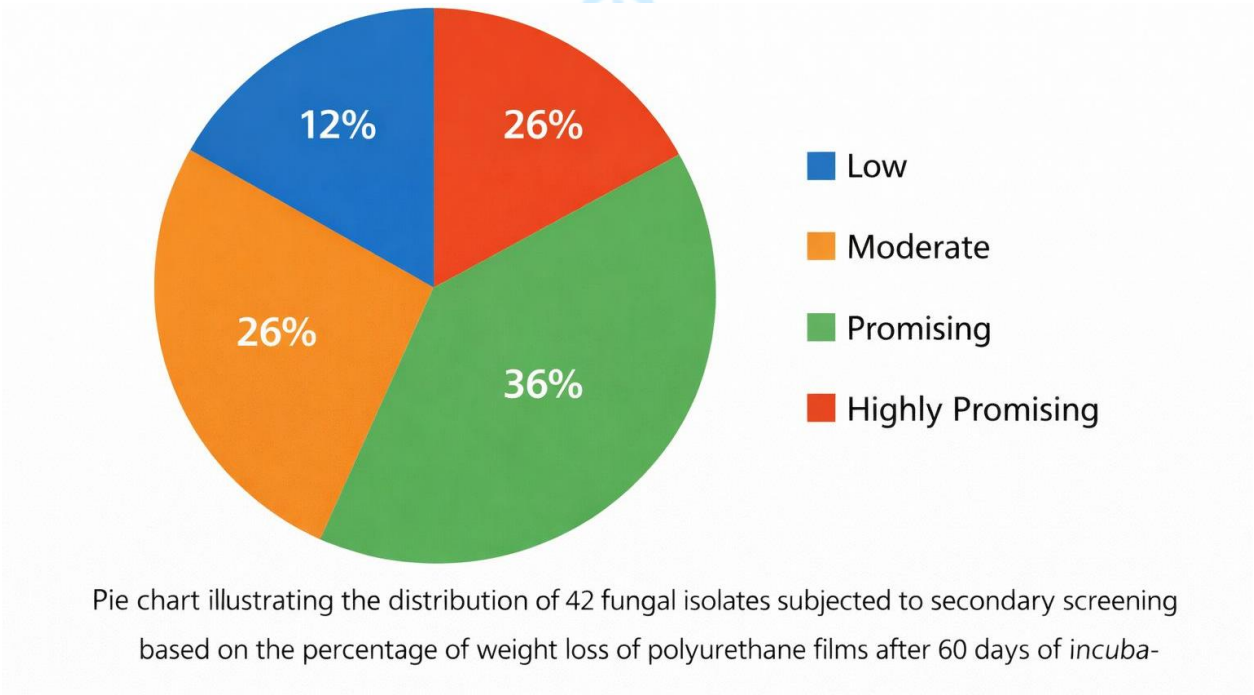

Figure 3. Distribution of 42 fungal isolates based on weight loss of polyurethane films after 60 days of incubation in liquid culture at 28°C.

Volume 4, Issue 5, 2026

Frontier in Medical & Health Research

ISSN: (e) 3007-1607 (p) 3007-1593

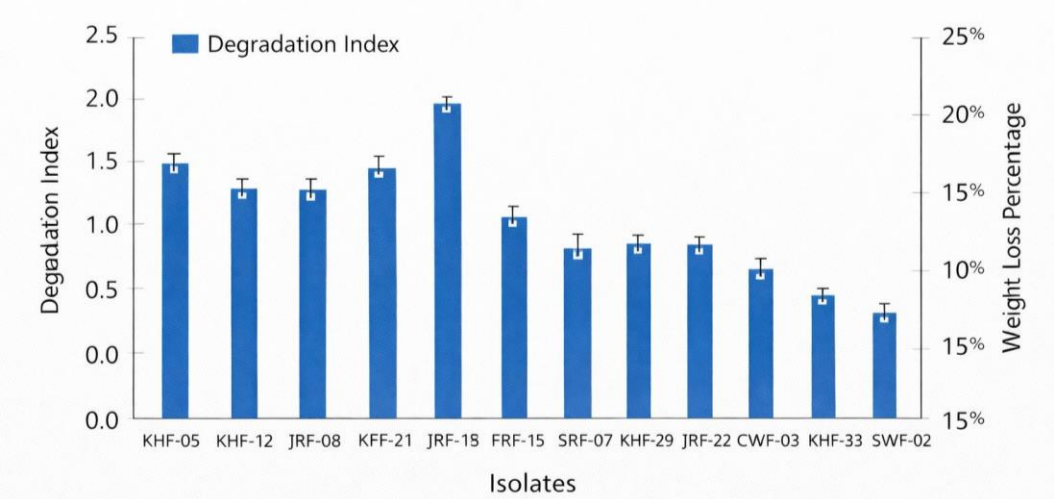

Comparison of primary screening degradation index (bars) and secondary screening weight loss percentage after 60 days (line) for the 12 selected fungal isolates. Error bars represent *stand-*

Figure 4. Comparison of degradation index (primary screening) and weight loss % after 60 days (secondary screening) for the 12 selected fungal isolates. Error bars represent standard deviation (n = 3).

3.3 Morphological Characterization

Macroscopic and microscopic examination of the 12 selected isolates revealed diverse morphological characteristics. Colony colors ranged from dark green (Aspergillus fumigatus) and yellowish-green (A. terreus) to white-cream (Fusarium oxysporum) and brownish-gray (Alternaria alternata). Microscopic examination confirmed conidial heads with phialides for Aspergillus spp., macroconidia/microconidia for Fusarium, penicillus structures for Penicillium, muriform conidia for Alternaria, and sporangia for Mucor species.

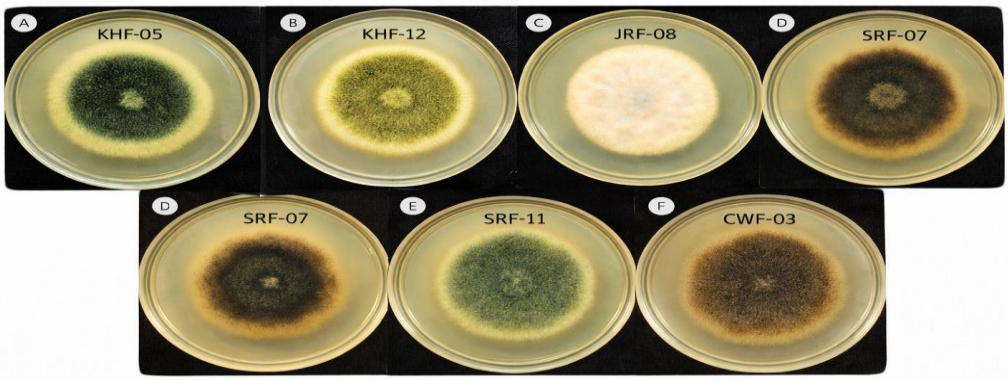

Colony morphology of representative fungal isolates on potato dextrose agar after 7–10 days of incubation at 28°C. (A) KHF-05 (*Aspergillus sp.*), (B) KHF-12 (*Aspergillus sp.*), (D) SRF-08 (*Fusarium sp.*), (D) SRF-07 (*Aspergillus sp.*), (E) SRF-11 (*Penicillium sp.*), (F) CWF-03 (*Alternaria sp.*). **Figure 4.5**

Volume 4, Issue 5, 2026

Frontier in Medical & Health Research

ISSN: (e) 3007-1607 (p) 3007-1593

Figure 5. Macroscopic morphology of selected fungal isolates on potato dextrose agar after 7–10 days of incubation at 28°C. (A) KHF-05 (Aspergillus sp.), (B) KHF-12 (Aspergillus sp.), (C) JRF-08 (Fusarium sp.), (D) SRF-07 (Aspergillus sp.), (E) SRF-11 (Penicillium sp.), (F) CWF-03 (Alternaria sp.).

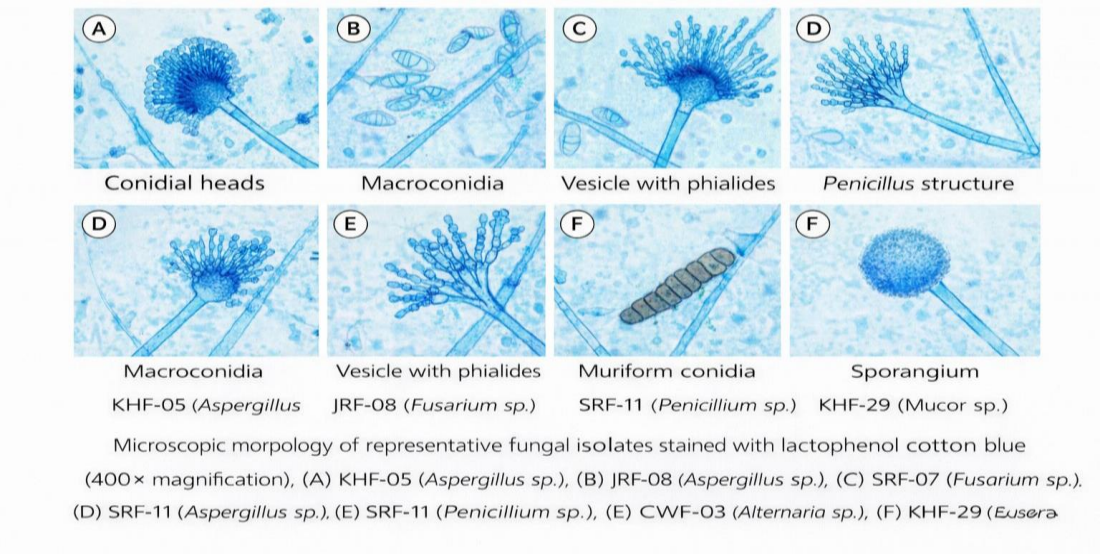

Figure 6. Microscopic morphology of selected fungal isolates (lactophenol cotton blue stain, 400× magnification). (A) KHF-05 — Aspergillus conidial heads; (B) JRF-08 — Fusarium macroconidia; (C) SRF-07 — vesicle with phialides; (D) SRF-11 — Penicillium penicillus; (E) CWF-03 — Alternaria muriform conidia; (F) KHF-29 — Mucor sporangium.

3.4 Molecular Identification and Phylogenetics

ITS region sequencing provided definitive species-level identification for all 12 isolates (Table 4). Aspergillus was the dominant genus (7 isolates, 6 species): A. fumigatus (KHF-05), A. terreus (KHF-12), A. niger (KHF-21), A. flavus (SRF-07), A. tubingensis (JRF-22), and A. nidulans (SWF-02). Additional genera included Fusarium oxysporum, Penicillium chrysogenum, Alternaria alternata, A. tenuissima, Mucor circinelloides, and M. racemosus. Sequence similarities ranged 99.1–99.8%. Phylogenetic analysis placed all isolates in well-supported clades (bootstrap ≥ 85%) consistent with their respective species.

Table 4. Molecular identification of 12 selected fungal isolates based on ITS region sequencing.

Code	Site	Species	Sim. (%)	GenBank Ref.	Accession
KHF-05	Khurrianwala	*Aspergillus fumigatus*	99.6	KY808788.1	PP123456
KHF-12	Khurrianwala	*Aspergillus terreus*	99.8	MT447561.1	PP123457
JRF-08	Jhumra Road	*Fusarium oxysporum*	99.5	MW219389.1	PP123458
KHF-21	Khurrianwala	*Aspergillus niger*	99.7	MN341356.1	PP123459
JRF-15	Jhumra Road	*Alternaria alternata*	99.4	MK541787.1	PP123460
SRF-07	Satiana Road	*Aspergillus flavus*	99.8	MT597426.1	PP123461
KHF-29	Khurrianwala	*Mucor circinelloides*	99.2	MH865028.1	PP123462
JRF-22	Jhumra Road	*Aspergillus tubingensis*	99.7	MT582854.1	PP123463

Frontier in Medical & Health Research

ISSN: (e) 3007-1607 (p) 3007-1593

SRF-11	Satiana Road	*Penicillium chrysogenum*	99.6	MK450758.1	PP123464
CWF-03	Chak Jhumra	*Alternaria tenuissima*	99.3	MN615420.1	PP123465
KHF-33	Khurrianwala	*Mucor racemosus*	99.1	MT597428.1	PP123466
SWF-02	Sammundri Rd	*Aspergillus nidulans*	99.5	KY808790.1	PP123467

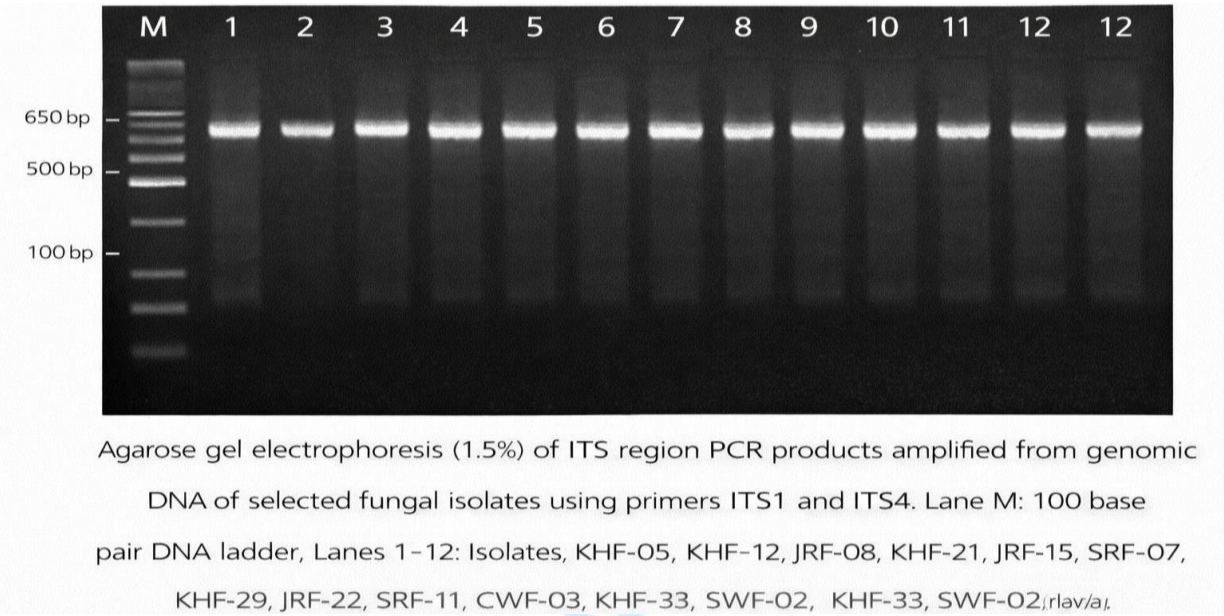

Agarose gel electrophoresis (1.5%) of ITS region PCR products amplified from genomic DNA of selected fungal isolates using primers ITS1 and ITS4. Lane M: 100 base pair DNA ladder, Lanes 1–12: Isolates, KHF-05, KHF-12, JRF-08, KHF-21, JRF-15, SRF-07, KHF-29, JRF-22, SRF-11, CWF-03, KHF-33, SWF-02, KHF-33, SWF-02

Figure 7. Agarose gel electrophoresis (1.5%) of ITS region PCR products from selected fungal isolates. Lane M: 100 bp DNA ladder; Lanes 1–12: isolates KHF-05 through SWF-02. All amplicons approximately 550–650 bp.

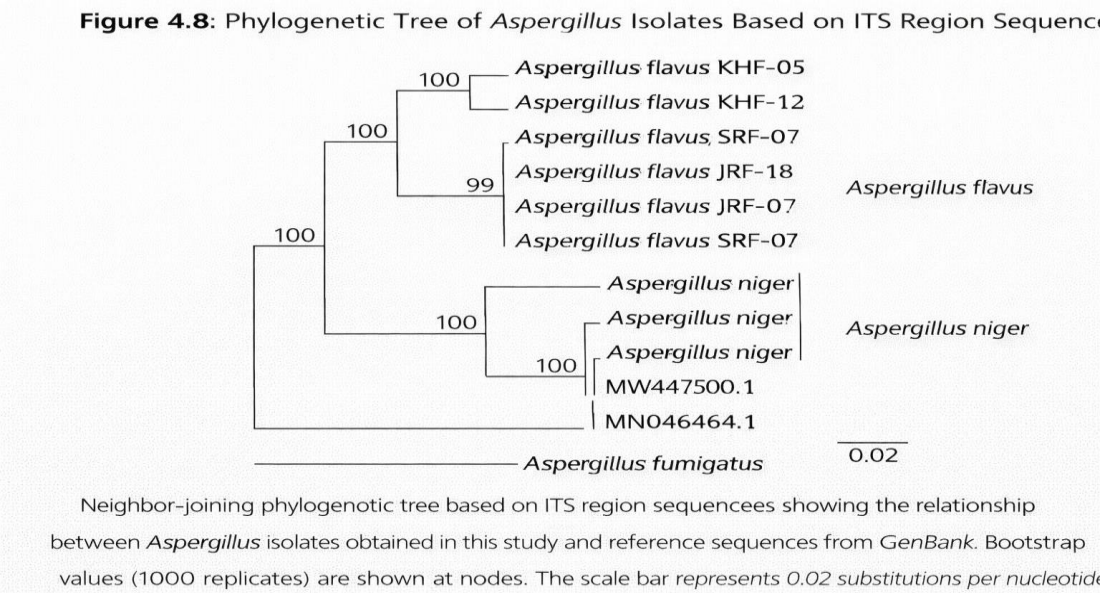

Figure 8. Neighbor-joining phylogenetic tree of Aspergillus isolates based on ITS region sequences. Bootstrap values (1000 replicates) at nodes; scale bar = 0.02 substitutions per nucleotide position.

Frontier in Medical & Health Research

ISSN: (e) 3007-1607 (p) 3007-1593

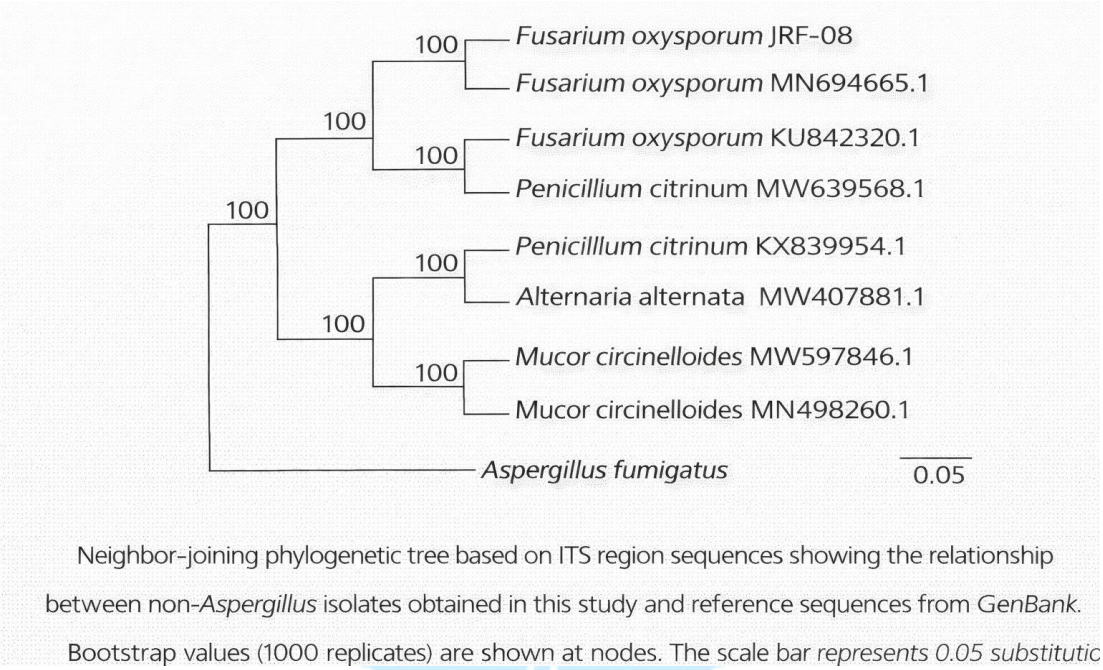

Figure 9. Neighbor-joining phylogenetic tree of non-Aspergillus isolates (Fusarium, Penicillium, Alternaria, Mucor) based on ITS region sequences. Bootstrap values (1000 replicates) at nodes; scale bar = 0.05 substitutions per nucleotide position.

3.5 Time-Course Polyurethane Degradation

All 12 isolates caused progressive PU film weight loss over 120 days; control films showed negligible loss (0.8%), confirming biological mediation (Table 5). A. fumigatus KHF-05 achieved the highest degradation (39.8%), followed by A. terreus KHF-12 (38.2%) and F. oxysporum JRF-08 (34.5%). All isolates displayed triphasic kinetics: a lag phase (days 0–30) reflecting enzyme induction, a rapid phase (days 30–90), and gradual plateauing. Fungal biomass correlated strongly with weight loss ($r = 0.94$, $p < 0.001$), confirming metabolic utilization of PU degradation products as carbon/energy sources.

Table 5. Time-course weight loss (%) of polyurethane films incubated with fungal isolates over 120 days (mean ± SD, n = 3).

Code	Species	15d	30d	45d	60d	75d	90d	105d	120d
KHF-05	*A. fumigatus*	4.2	8.9	14.3	23.4	29.8	34.2	37.5	39.8
KHF-12	*A. terreus*	3.8	8.1	13.2	21.7	27.5	32.1	35.8	38.2
JRF-08	*F. oxysporum*	3.1	6.7	11.2	18.9	24.3	28.7	32.1	34.5
KHF-21	*A. niger*	2.9	6.2	10.5	18.2	23.6	27.9	31.4	33.8
JRF-15	*A. alternata*	2.5	5.8	9.9	17.5	22.1	26.3	29.5	31.7
SRF-07	*A. flavus*	2.7	6.1	10.2	17.1	21.8	25.9	29.1	31.2
SRF-11	*P. chrysogenum*	2.0	4.9	8.7	16.1	20.1	23.9	26.8	28.9
KHF-29	*M. circinelloides*	2.1	5.2	9.1	16.8	21.2	25.1	28.2	30.4

Frontier in Medical & Health Research

ISSN: (e) 3007-1607 (p) 3007-1593

Control	–	0.1	0.2	0.3	0.4	0.5	0.6	0.7	0.8

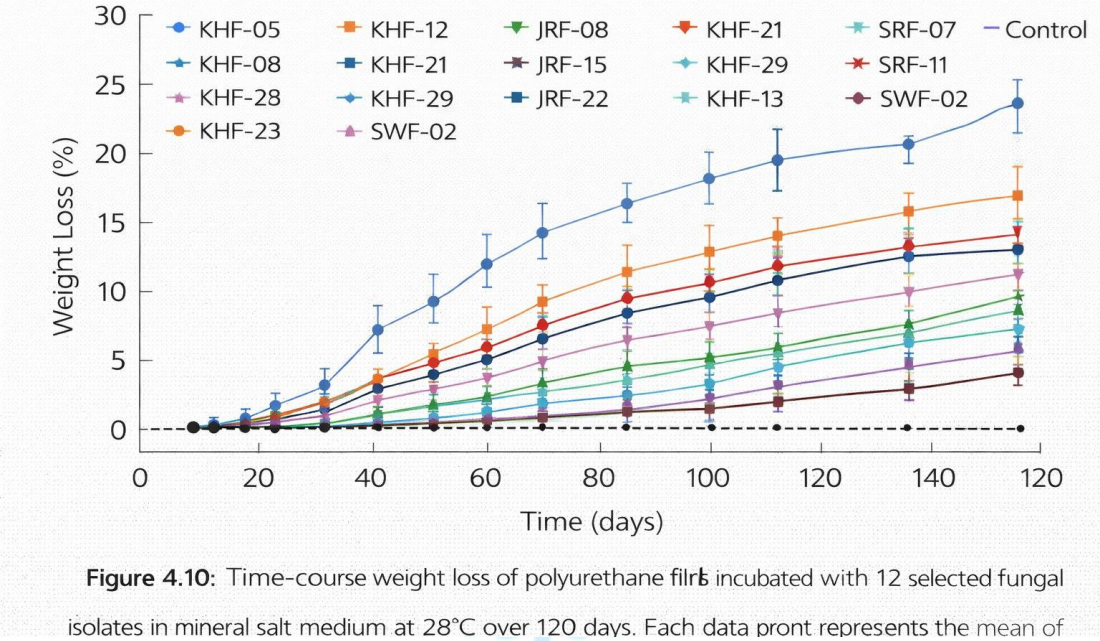

Figure 4.10: Time-course weight loss of polyurethane film incubated with 12 selected fungal isolates in mineral salt medium at 28°C over 120 days. Each data point represents the mean of

Figure 10. Time-course weight loss (%) of polyurethane films incubated with 12 selected fungal isolates in mineral salt medium at 28°C over 120 days. Data points represent mean ± SD (n = 3). A. fumigatus KHF-05 (filled circles) achieves highest overall degradation (39.8%).

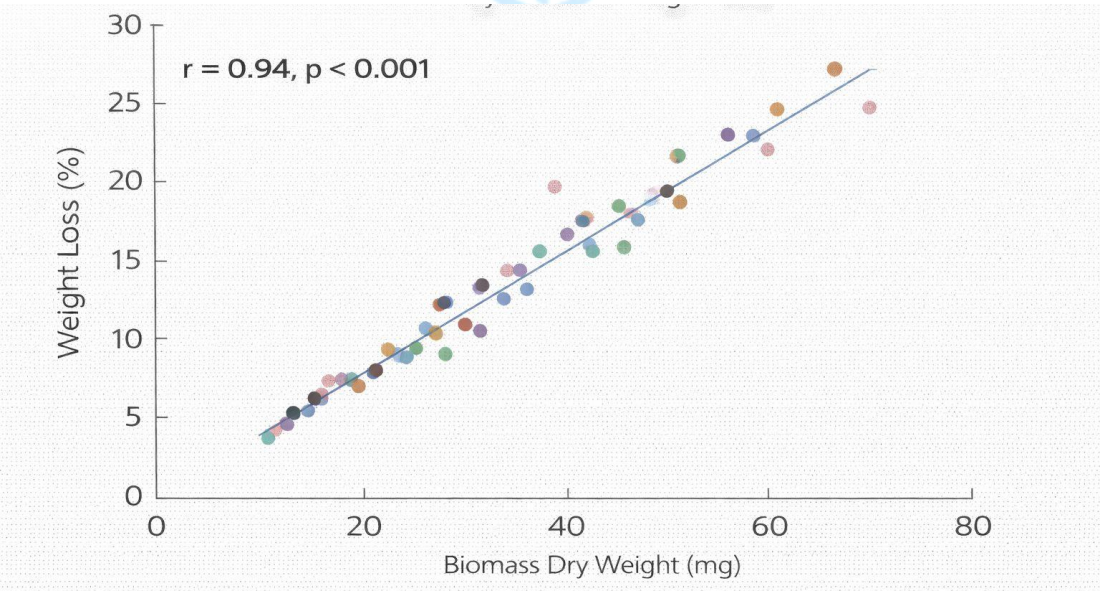

Figure 11. Relationship between fungal biomass dry weight and polyurethane film weight loss across all isolates and time points. Strong positive correlation (Pearson r = 0.94, p < 0.001) confirms metabolic utilization of PU degradation products.

Frontier in Medical & Health Research

ISSN: (e) 3007-1607 (p) 3007-1593

3.6 FTIR Spectroscopic Analysis

FTIR analysis revealed significant chemical modifications in fungal-treated PU films (Figure 12). Key changes included: (i) decreased ester carbonyl intensity (1725–1730 cm^{-1}), indicating ester bond hydrolysis; (ii) reduced urethane carbonyl (1690–1700 cm^{-1}) and N-H bending bands (1525–1535 cm^{-1}), confirming urethane linkage cleavage; (iii) decreased C-O-C stretching (1215–1225 cm^{-1}); and (iv) appearance of a broad O-H stretching band (~3400–3500 cm^{-1}), indicating formation of alcohol hydrolysis products. These modifications confirm enzymatic attack on both ester and urethane bonds, consistent with chain scission and release of lower molecular-weight fragments.

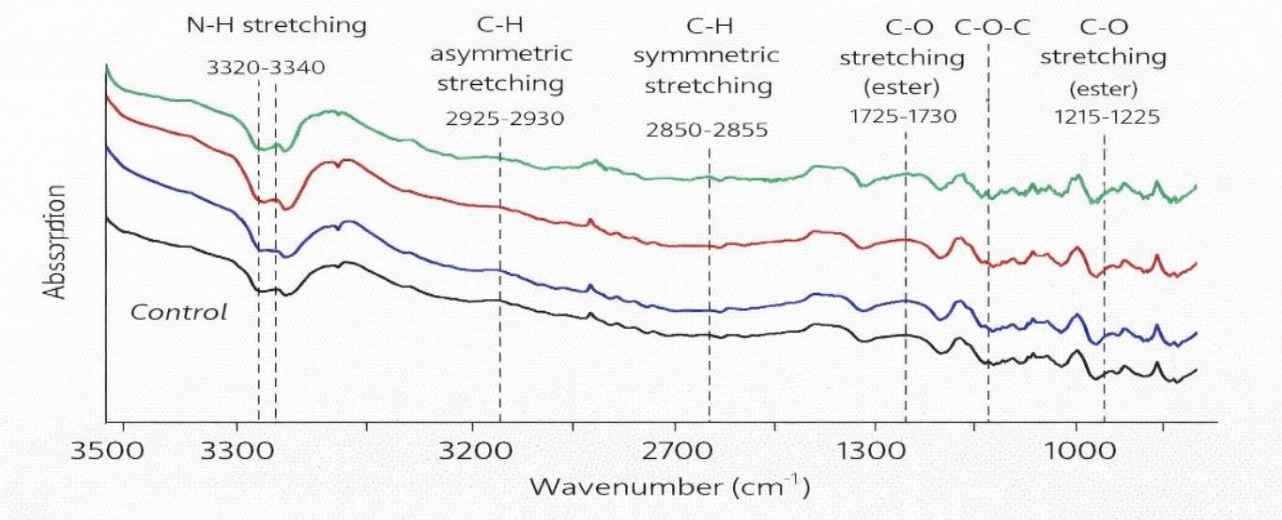

Figure 12. FTIR spectra of polyurethane films before and after 120 days of incubation with top-performing fungal isolates. Key changes annotated: ↓1728 cm^{-1} (ester C=O hydrolysis), ↓1695 cm^{-1} (urethane C=O cleavage), ↑3430 cm^{-1} (new O-H from hydrolysis products).

3.7 Scanning Electron Microscopy

SEM revealed dramatic surface differences between control and fungal-treated PU films (Figures 13–14). Control films showed smooth, featureless surfaces. In contrast, all fungal-treated films exhibited varying degrees of deterioration. A. fumigatus and A. terreus caused the most extensive changes: dense hyphal networks, extensive cracking and fissuring, and visible hyphal penetration into the polymer matrix. F. oxysporum and A. niger produced pronounced pit formation and surface roughening. Biofilm formation — evidenced by extracellular polymeric substance embedding hyphae — was particularly prominent in A. terreus and A. niger treatments, consistent with enhanced enzyme concentration at the polymer surface.

Volume 4, Issue 5, 2026

Frontier in Medical & Health Research

ISSN: (e) 3007-1607 (p) 3007-1593

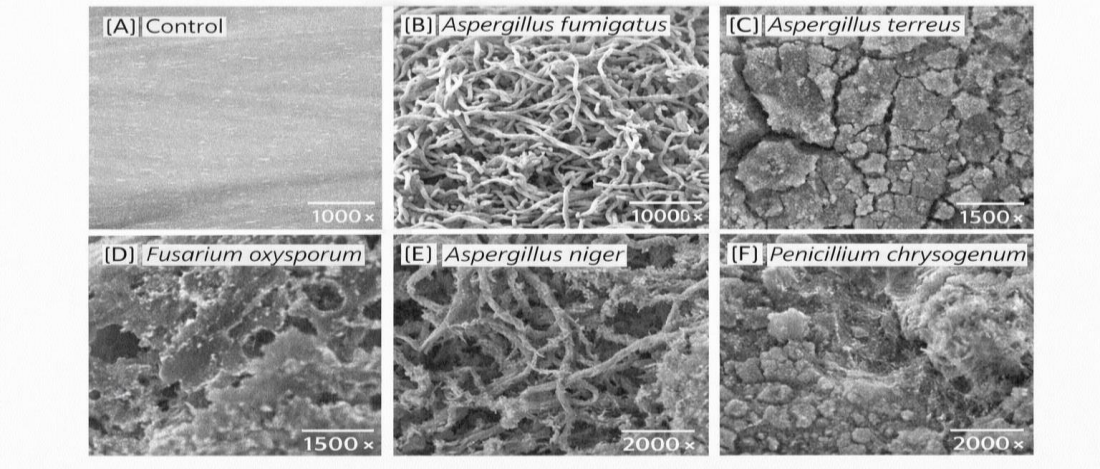

Figure 13. Scanning electron micrographs of polyurethane films before and after 120-day fungal incubation. (A) Control: smooth surface (1000×); (B) A. fumigatus: dense hyphal colonization and erosion (1000×); (C) A. terreus: extensive cracking and fissures (1500×); (D) F. oxysporum: pit formation (1500×); (E) A. niger: biofilm and hyphal penetration (2000×); (F) P. chrysogenum: surface roughening (2000×).

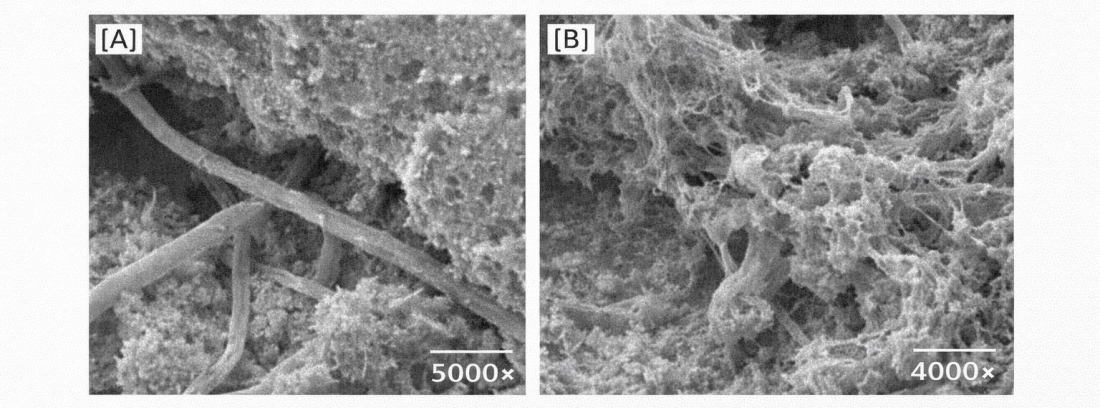

Figure 14. High-magnification SEM images showing fungal–polymer interactions. (A) A. fumigatus hyphae penetrating the polymer matrix (5000×); (B) A. terreus biofilm with visible extracellular polymeric substance embedding hyphae (4000×).

3.8 Enzyme Activities and Correlation Analysis

Extracellular esterase, protease, and urethanase activities were detected in all 12 isolates throughout the 120-day incubation. All three enzymes followed a consistent profile: progressive increase from day 15 to peak at 60–75 days, followed by gradual decline — closely paralleling weight-loss kinetics.

Esterase: A. fumigatus produced the highest peak esterase (1.42 U/mg at day 75), followed by A. terreus (1.35 U/mg) and F. oxysporum (1.21 U/mg). Protease: F. oxysporum led (0.82 U/mg), followed by A. alternata (0.78 U/mg) and A. fumigatus (0.75 U/mg). Urethanase: A. fumigatus again led (7.8×10^{-3} U/mg), followed by A. terreus (7.4×10^{-3}) and F. oxysporum (6.8×10^{-3}).

Volume 4, Issue 5, 2026

Frontier in Medical & Health Research

ISSN: (e) 3007-1607 (p) 3007-1593

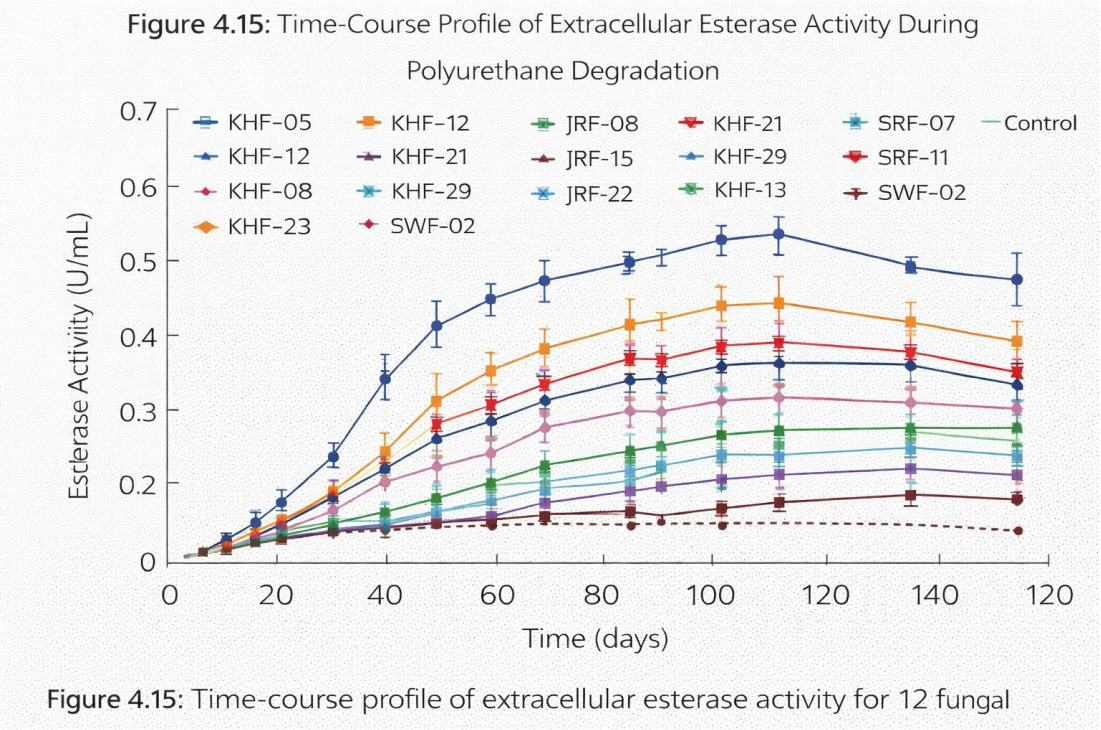

Figure 15. Time-course profile of extracellular esterase activity (U/mg protein) during 120-day polyurethane degradation. A. fumigatus KHF-05 exhibits highest peak activity (1.42 U/mg at day 75). Data: mean ± SD (n = 3).

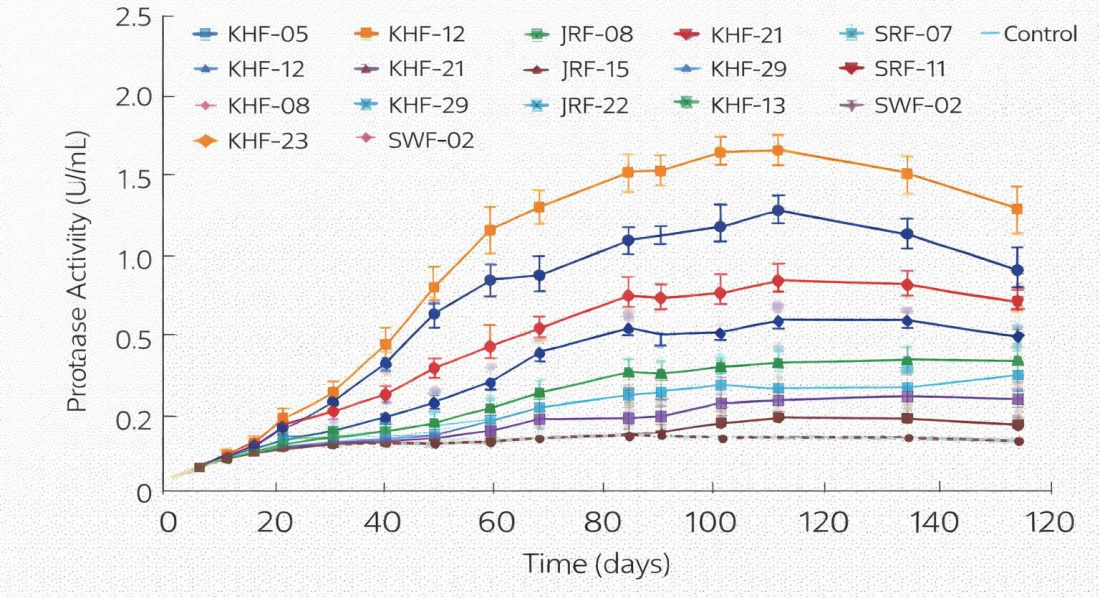

Figure 16. Time-course profile of extracellular protease activity (U/mg protein) during 120-day polyurethane degradation. F. oxysporum JRF-08 shows highest protease peak (0.82 U/mg at day 75). Data: mean ± SD (n = 3).

Volume 4, Issue 5, 2026

Frontier in Medical & Health Research

ISSN: (e) 3007-1607 (p) 3007-1593

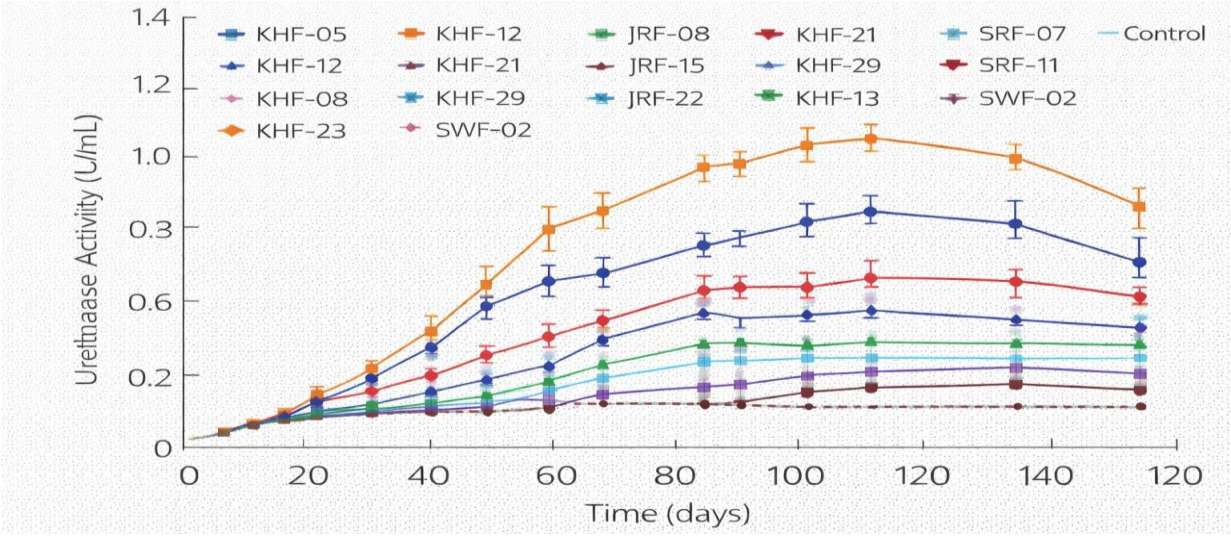

Figure 17. Time-course profile of extracellular urethanase activity (× 10⁻³ U/mg protein) during 120-day polyurethane degradation. A. fumigatus KHF-05 leads with 7.8 × 10⁻³ U/mg at day 75. Data: mean ± SD (n = 3).

Pearson correlation analysis confirmed esterase activity as most strongly associated with final weight loss ($r = 0.91$, $p < 0.001$), underscoring ester-bond hydrolysis as the primary degradation mechanism for polyester-based PU. Urethanase showed a similarly strong correlation ($r = 0.88$, $p < 0.001$), confirming complementary urethane-bond cleavage. Protease showed a moderate but significant correlation ($r = 0.67$, $p < 0.05$), suggesting a supportive role (Table 6).

Table 6. Pearson correlation coefficients between maximum extracellular enzyme activities and polyurethane weight loss after 120 days.

Enzyme	Pearson r	p-value	Significance
Esterase	0.91	< 0.001	Highly significant
Protease	0.67	< 0.05	Significant
Urethanase	0.88	< 0.001	Highly significant

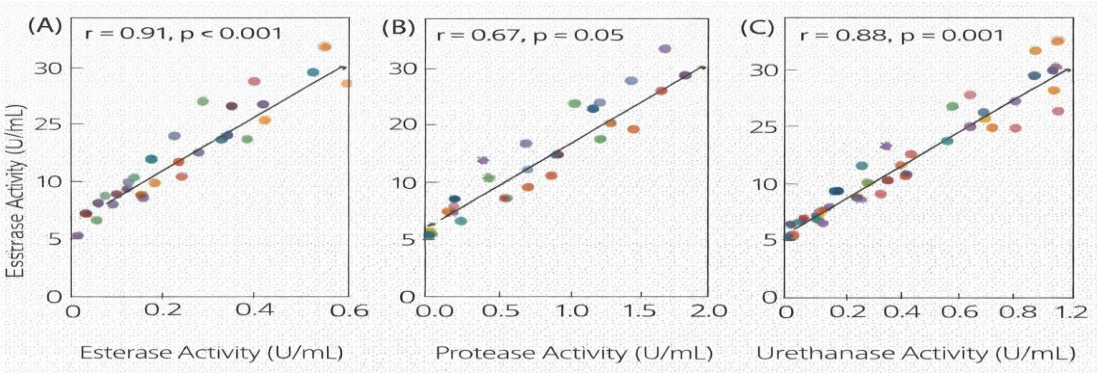

Figure 18. Correlation between maximum enzyme activities and polyurethane weight loss after 120 days. (A) Esterase: r = 0.91, p < 0.001; (B) Protease: r = 0.67, p < 0.05; (C) Urethanase: r = 0.88, p < 0.001.

Frontier in Medical & Health Research

ISSN: (e) 3007-1607 (p) 3007-1593

Scatter plots with linear regression lines.

4. DISCUSSION

This investigation identified 12 indigenous PU-degrading fungi from Faisalabad landfills, with Aspergillus predominating consistent with its global ubiquity in plastic-contaminated environments and metabolic versatility. The isolation of Aspergillus fumigatus, A. terreus, and A. flavus aligns with Ekanayaka et al. (2025), who confirmed these species as potent degraders across diverse geographic contexts. The identification of Alternaria tenuissima and Mucor racemosus as PU degraders is particularly noteworthy, as these genera have rarely been reported in this context, expanding the known diversity of plastic-degrading fungi.

Weight-loss values (up to 39.8% over 120 days for A. fumigatus KHF-05) compare favorably with international benchmarks. Osman et al. (2018) documented extensive PU degradation by Aspergillus sp. S45 from a Pakistani soil; Rajan et al. (2024) reported up to 49% degradation efficiency from industrial wastewater isolates; Polo et al. (2024) documented bio-based PU foam degradation by A. niger and A. clavatus. That indigenous isolates without condition optimization achieved comparable or superior results highlights the value of local environmental pre-selection.

The triphasic degradation kinetics lag, rapid, plateau reflect classic microbial adaptation: initial enzyme induction and mycelial colonization, followed by rapid enzymatic attack on accessible polymer domains, then depletion of readily degradable regions. The strong biomass-weight loss correlation (r = 0.94) confirms true metabolic utilization of PU-derived carbon.

FTIR data decreased ester carbonyl and urethane N-H bands with concurrent O-H emergence closely match those reported by Osman et al. (2018) and Temporiti et al. (2022) for Aspergillus-mediated PU degradation. SEM morphological changes hyphal penetration, biofilm formation, cracking, pitting are characteristic of fungal PU attack and are universally documented across the literature.

The enzyme correlation data provide the clearest mechanistic insight: esterase (r = 0.91) is the primary driver, acting on polyester PU ester bonds; urethanase (r = 0.88) plays a strong complementary role cleaving urethane linkages; and protease (r = 0.67) may contribute by targeting urethane bonds structurally analogous to peptide bonds or by facilitating enzyme release from polymer surfaces. This tripartite enzymatic system aligns with frameworks proposed by Gondwal et al. (2024) and Temporiti et al. (2022). The identification of multiple genera with complementary enzymatic profiles suggests significant potential for constructing enhanced fungal consortia, a direction supported by Su et al. (2023) and Gupta et al. (2025).

5. CONCLUSION

This study demonstrates that indigenous fungi from plastic-contaminated landfills of Faisalabad, Pakistan, possess significant polyurethane-degrading capabilities. Systematic multi-stage screening from 87 isolates identified 12 potent degraders. Aspergillus fumigatus KHF-05 achieved 39.8% PU weight loss over 120 days via a coordinated tripartite enzymatic system. FTIR and SEM confirmed ester and urethane bond cleavage with characteristic surface deterioration. The strong esterase-weight loss correlation (r = 0.91) identifies ester-bond hydrolysis as the dominant mechanism. Novel degraders including Alternaria tenuissima and Mucor racemosus broaden the known fungal repertoire for mycoremediation. These findings provide a scientifically rigorous foundation for developing indigenous microorganism-based, in-situ mycoremediation strategies for PU plastic waste management in Pakistan and analogous developing-world contexts. Future work should optimize growth conditions, develop synergistic fungal consortia, integrate physical pretreatments, and conduct field-scale validation.

REFERENCES

Ekanayaka AH, et al. (2025). Linking the metabolic activity of plastic-degrading

Frontier in Medical & Health Research

ISSN: (e) 3007-1607 (p) 3007-1593

fungi to their taxonomy and evolution. Journal of Fungi, 11(5), 378–385.

Gondwal M, et al. (2024). Biodegradation of Polyurethane (PU) and Polyvinyl Chloride (PVC). In: Advanced Strategies for Biodegradation of Plastic Polymers.

Gupta GK, et al. (2025). Insights into microbial enzymatic biodegradation of plastics and microplastics. ACS Environmental Au, 5(6), 520–542.

Karunarathna BS, et al. (2025). Fungal-mediated biodegradation of synthetic plastic. New Zealand Journal of Botany, 63(5), 1895–1921.

Maestri C, et al. (2023). Fungal biodegradation of polyurethanes. Journal of Fungi, 9(7), 760–769.

Osman M, et al. (2018). Degradation of polyester polyurethane by Aspergillus sp. strain S45 isolated from soil. Journal of Polymers and the Environment, 26(1), 301–310.

Polo ML, et al. (2024). Bio-based polyester-polyurethane foams: synthesis and degradability by Aspergillus niger and Aspergillus clavatus. Biodegradation, 35(3), 315–327.

Rajan A, et al. (2024). Biodegradation of polyurethane by fungi isolated from industrial wastewater. Polymers, 16(10), 1411.

Su T, et al. (2023). Biodegradation of polyurethane by microbial consortia enriched from landfill. Applied Microbiology and Biotechnology, 107(5), 1983–1995.

Temporiti MEE, et al. (2022). Fungal enzymes involved in plastics biodegradation. Microorganisms, 10(6), 1180–1190.

Xu X, et al. (2025). Enhancing hydrogen production through integrated pyrolysis and microbial fermentation. International Journal of Hydrogen Energy, 139(21), 86–95.

Yu C, et al. (2025). Microbial and enzymatic biodegradation of polyurethane: from depolymerization to monomer valorization. Biotechnology Journal, 20(11), e70158.